

# COLD SCALAR-TENSOR BLACK HOLES: CAUSAL STRUCTURE, GEODESICS, STABILITY

K.A. Bronnikov<sup>1</sup>, G. Clément<sup>2</sup>, C.P. Constantinidis<sup>3</sup> and J.C. Fabris<sup>4</sup>

*Departamento de Física, Universidade Federal do Espírito Santo, Vitória, Espírito Santo, Brazil*

We study the structure and stability of the recently discussed spherically symmetric Brans-Dicke black-hole type solutions with an infinite horizon area and zero Hawking temperature, existing for negative values of the coupling constant  $\omega$ . These solutions split into two classes: B1, whose horizon is reached by an infalling particle in a finite proper time, and B2, for which this proper time is infinite. Class B1 metrics are shown to be extendable beyond the horizon only for discrete values of mass and scalar charge, depending on two integers  $m$  and  $n$ . In the case of even  $m - n$  the space-time is globally regular; for odd  $m$  the metric changes its signature as the horizon is crossed. Nevertheless, the Lorentzian nature of the space-time is preserved, and geodesics are smoothly continued across the horizon, but, when crossing the horizon, for odd  $m$  timelike geodesics become spacelike and *vice versa*. Problems with causality, arising in some cases, are discussed. Tidal forces are shown to grow infinitely near type B1 horizons. All vacuum static, spherically symmetric solutions of the Brans-Dicke theory with  $\omega < -3/2$  are found to be linearly stable against spherically symmetric perturbations. This result extends to the generic case of the Bergmann-Wagoner class of scalar-tensor theories of gravity with the coupling function  $\omega(\phi) < -3/2$ .

## 1. Introduction

In the recent years there has been a renewed interest in scalar-tensor theories (STT) of gravity as viable alternatives to general relativity (GR), mostly in connection with their possible role in the early Universe: they provide power-law instead of exponential inflation, leading to more plausible perturbation spectra [1]. Another aspect of interest in STT is the possible existence of black holes (BHs) different from those well-known in GR. Thus, Campanelli and Lousto [2] pointed out among the static, spherically symmetric solutions of the Brans-Dicke (BD) theory a subfamily possessing all BH properties, but (i) existing only for negative values of the coupling constant  $\omega$  and (ii) with horizons of infinite area. These authors argued that large negative  $\omega$  are compatible with modern observations and that such BHs may be of astrophysical

relevance<sup>5</sup>. Indeed, the post-Newtonian parameters, determining the observational behaviour of STT in the weak field limit, depend crucially on the absolute value of  $\omega$  rather than its sign [4, 5].

In Ref. [3] it was shown, in the framework of a general (Bergmann-Wagoner) class of STT, that nontrivial BH solutions can exist for the coupling function  $\omega(\phi) + 3/2 < 0$ , and that only in exceptional cases these BHs have a finite horizon area. In the BD theory ( $\omega = \text{const}$ ) such BHs were indicated explicitly; they have infinite horizon areas and zero Hawking temperature (“cold BHs”), thus confirming the conclusions of [2]. These BHs in turn split into two subclasses: B1, where horizons are attained by infalling particles in a finite proper time  $\tau$ , and B2, for which  $\tau$  is infinite. These results are briefly presented in Sections 2 and 3.

The static region of a type B2 BH is geodesically complete since its horizon is infinitely remote and actually forms a second spatial asymptotic. For type B1 BHs the global picture is more complex and is discussed here in some detail (Sec. 4). It turns out that the horizon is generically singular due to violation of analyticity, despite the vanishing curvature invariants. Only a discrete set of B1-solutions, parametrized by

<sup>1</sup>e-mail: kb@goga.mainet.msk.su; permanent address: Centre for Gravitation and Fundamental Metrology, VNIIMS, 3-1 M. Ulyanovoy St., Moscow 117313, Russia.

<sup>2</sup>e-mail: gecl@ccr.jussieu.fr; permanent address: Laboratoire de Gravitation et Cosmologie Relativistes, Université Pierre et Marie Curie, CNRS/URA769, Tour 22-12, Boîte 142, 4 Place Jussieu, 75252 Paris Cedex 05, France.

<sup>3</sup>e-mail: clisthen@cce.ufes.br

<sup>4</sup>e-mail: fabris@cce.ufes.br

<sup>5</sup>For brevity, we call BHs with infinite horizon areas type B BHs [3], to distinguish them from the conventional ones, with finite horizon areas, to be called type A.

two integers  $m$  and  $n$ , admits a Kruskal-like extension, and, depending on their parity, four different global structures are distinguished. Two of them, where  $m-n$  is even, are globally regular, in two others the region beyond the horizon contains a spacelike singularity.

Subsec. 4.4 describes the behaviour of geodesics for different cases of BD BH metrics. It turns out that for odd  $m$ , when crossing the horizon, timelike geodesics become spacelike and *vice versa*, leading to problems with causality. Thus, in a family of BHs there appear closed timelike curves, whose existence may be avoided by assuming a ‘‘helical’’ analytic extension of the space-time manifold. Moreover, it is shown by considering the geodesic deviation equations that near a horizon with an infinite area all extended bodies are destroyed (stretched apart) by unbounded tidal forces.

Sec. 5 discusses the stability of STT solutions under spherically symmetric perturbations. In this case the only dynamical degree of freedom is the scalar field, and the perturbation analysis reduces to a single wave equation whose radial part determines the system behaviour. Under reasonable boundary conditions, it turns out that the BD solutions with  $\omega < -3/2$  are linearly stable, and this result extends to similar solutions of the general STT provided the scalar field does not create new singularities in the static domain. For the case  $\omega > -3/2$  the stability conclusion depends on the boundary condition at a naked singularity, which is hard to formulate unambiguously.

We can conclude that, in STT with the anomalous sign of the scalar field energy, vacuum spherically symmetric solutions generically describe stable BH-like configurations. Some of them, satisfying a ‘‘quantization’’ condition, are globally regular and have peculiar global structures. We also conclude that, due to infinite tidal forces, a horizon with an infinite area converts any infalling body into true elementary (point-like) particles, which afterwards become tachyons.

A short preliminary account of this work has been given in [7]. In our next paper we intend to discuss similar solutions with an electric charge.

## 2. Field equations

The Lagrangian of the general (Bergmann-Wagoner) class of STT of gravity in four dimensions is

$$L = \sqrt{-g} \left[ \phi R + \frac{\omega(\phi)}{\phi} \phi_{;\rho} \phi^{;\rho} + L_m \right] \quad (1)$$

where  $\omega(\phi)$  is an arbitrary function of the scalar field  $\phi$  and  $L_m$  is the Lagrangian of non-gravitational matter. This formulation (the so-called *Jordan conformal frame*) is commonly considered to be fundamental since just in this frame the matter energy-momentum

tensor  $T_\nu^\mu$  obeys the conventional conservation law  $\nabla_\alpha T_\mu^\alpha = 0$ , giving the usual equations of motion (the so-called atomic system of measurements). In particular, free particles move along geodesics of the Jordan-frame metric. Therefore, in what follows we discuss the geometry, causal structure and geodesics in the Jordan frame.

We consider only scalar-vacuum configurations and put  $L_m = 0$ .

The field equations are easier to deal with in the *Einstein conformal frame*, where the transformed scalar field  $\varphi$  is minimally coupled to gravity. Namely, the conformal mapping  $g_{\mu\nu} = \phi^{-1} \bar{g}_{\mu\nu}$  transforms Eq. (1) (up to a total divergence) to

$$L = \sqrt{-\bar{g}} \left( \bar{R} + \varepsilon \bar{g}^{\alpha\beta} \varphi_{;\alpha} \varphi_{;\beta} \right), \quad (2)$$

$$\varepsilon = \text{sign}(\omega + 3/2), \quad \frac{d\varphi}{d\phi} = \left| \frac{\omega + 3/2}{\phi^2} \right|^{1/2}. \quad (3)$$

The field equations are

$$R_{\mu\nu} = -\varepsilon \varphi_{;\mu} \varphi_{;\nu}, \quad \nabla^\alpha \nabla_\alpha \varphi = 0 \quad (4)$$

where we have suppressed the bars marking the Einstein frame. The value  $\varepsilon = +1$  corresponds to normal STT, with positive energy density in the Einstein frame; the choice  $\varepsilon = -1$  is anomalous. The BD theory corresponds to the special case  $\omega = \text{const}$ , so that

$$\phi = \exp(\varphi / \sqrt{|\omega + 3/2|}). \quad (5)$$

Let us consider a spherically symmetric field system, with the metric

$$ds_E^2 = e^{2\gamma} dt^2 - e^{2\alpha} du^2 - e^{2\beta} d\Omega^2, \quad (6)$$

$$d\Omega^2 = d\theta^2 + \sin^2 \theta d\Phi^2,$$

where E stands for the Einstein frame,  $u$  is the radial coordinate,  $\alpha$ ,  $\beta$ ,  $\gamma$  and the field  $\varphi$  are functions of  $u$  and  $t$ . Preserving only linear terms with respect to time derivatives, we can write Eqs. (4) in the following form:

$$e^{2\alpha} R_0^0 = e^{2\alpha-2\gamma} (\ddot{\alpha} + 2\ddot{\beta}) - [\gamma'' + \gamma'(\gamma' - \alpha' + 2\beta')] = 0; \quad (7)$$

$$e^{2\alpha} R_1^1 = e^{2\alpha-2\gamma} \ddot{\alpha} - [\gamma'' + 2\beta'' + \gamma'^2 + 2\beta'^2 - \alpha'(\gamma' + 2\beta')] = \frac{1}{2} \varepsilon \dot{\varphi}^2; \quad (8)$$

$$e^{2\alpha} R_2^2 = e^{2\alpha-2\beta} + e^{2\alpha-2\gamma} \ddot{\beta} - [\beta'' + \beta'(\gamma' - \alpha' + 2\beta')] = 0; \quad (9)$$

$$R_{01} = 2[\dot{\beta}' + \dot{\beta}\beta' - \dot{\alpha}\beta' - \dot{\beta}\gamma'] = -\varepsilon \dot{\varphi} \varphi'; \quad (10)$$

$$\sqrt{-g} \square \varphi = e^{-\gamma+\alpha+2\beta} \ddot{\varphi} - (e^{\gamma-\alpha+2\beta} \varphi')' = 0 \quad (11)$$

where dots and primes denote, respectively,  $\partial/\partial t$  and  $\partial/\partial u$ .

Up to the end of Sec. 4 we will restrict ourselves to static configurations.

### 3. Black holes in scalar-tensor theories

The general static, spherically symmetric scalar-vacuum solution of the theory (1) is given by [4, 6]

$$ds_J^2 = \frac{1}{\phi} ds_E^2 = \frac{1}{\phi} \left\{ e^{-2bu} dt^2 - \frac{e^{2bu}}{s^2(k, u)} \left[ \frac{du^2}{s^2(k, u)} + d\Omega^2 \right] \right\}, \quad (12)$$

$$\varphi = Cu + \varphi_0, \quad C, \varphi_0 = \text{const}, \quad (13)$$

where J denotes the Jordan frame,  $u$  is the harmonic radial coordinate in the static space-time in the Einstein frame, such that  $\alpha(u) = 2\beta(u) + \gamma(u)$ , and the function  $s(k, u)$  is

$$s(k, u) \stackrel{\text{def}}{=} \begin{cases} k^{-1} \sinh ku, & k > 0, \\ u, & k = 0, \\ k^{-1} \sin ku, & k < 0, \end{cases} \quad (14)$$

The constants  $b$ ,  $k$  and  $C$  (the scalar charge) are related by

$$2k^2 \text{sign } k = 2b^2 + \varepsilon C^2. \quad (15)$$

The range of  $u$  is  $0 < u < u_{\text{max}}$ , where  $u = 0$  corresponds to spatial infinity, while  $u_{\text{max}}$  may be finite or infinite depending on  $k$  and the behaviour of  $\phi(\varphi)$  described by (3). In normal STT ( $\varepsilon = +1$ ), by (15), we have only  $k > 0$ , while in anomalous STT  $k$  can have either sign.

According to the previous studies [4, 6], all these solutions in normal STT have naked singularities, up to rare exceptions when the sphere  $u = \infty$  is regular and admits an extension of the static coordinate chart. An example is a conformal scalar field in GR viewed as a special case of STT, leading to BHs with scalar charge [8, 9]. Even when it is the case, such configurations are unstable due to blowing-up of the effective gravitational coupling [10].

In anomalous STT ( $\varepsilon = -1$ ) the solution behaviour is more diverse and the following cases without naked singularities can be found:

**1.  $k > 0$ .** Possible event horizons have an infinite area (type B BHs), i.e.  $g_{22} \rightarrow \infty$  as  $r \rightarrow 2k$ . In BD theory, after the coordinate transformation

$$e^{-2ku} = 1 - 2k/r \equiv P(r) \quad (16)$$

the solution takes the form

$$\begin{aligned} ds_J^2 &= P^{-\xi} ds_E^2 \\ &= P^{-\xi} \left( P^a dt^2 - P^{-a} dr^2 - P^{1-a} r^2 d\Omega^2 \right), \\ \phi &= P^\xi \end{aligned} \quad (17)$$

with the constants related by

$$(2\omega + 3)\xi^2 = 1 - a^2, \quad a = b/k. \quad (18)$$

The allowed range of  $a$  and  $\xi$ , providing a horizon without a curvature singularity at  $r = 2k$ , is

$$a > 1, \quad a > \xi \geq 2 - a. \quad (19)$$

(Eqs. (17),(18) are valid for  $\omega > -3/2$  as well, but then  $a < 1$ , leading to a naked singularity.)

For  $\xi < 1$  particles can arrive at the horizon in a finite proper time and may eventually (if geodesics can be extended) cross it, entering the BH interior (type B1 BHs [3]). When  $\xi \geq 1$ , the sphere  $r = 2k$  is infinitely far and it takes an infinite proper time for a particle to reach it. Since in the same limit  $g_{22} \rightarrow \infty$ , this configuration (a type B2 BH [3]) resembles a wormhole.

**2.  $k = 0$ .** Just as for  $k > 0$ , in a general STT, only type B black holes are possible [3]), with  $g_{22} \rightarrow \infty$  as  $u \rightarrow \infty$ . In particular, the BD solution is

$$\begin{aligned} ds^2 &= e^{-su} \left[ e^{-2bu} dt^2 - \frac{e^{2bu}}{u^2} \left( \frac{du^2}{u^2} + d\Omega^2 \right) \right], \\ \phi &= e^{su}, \quad s^2(\omega + 3/2) = -2b^2. \end{aligned} \quad (20)$$

The allowed range of the integration constants is  $b > 0$ ,  $2b > s > -2b$ . This range is again divided into two halves: for  $s > 0$  we deal with a type B1 BH, for  $s < 0$  with that of type B2 ( $s = 0$  is excluded since it leads to GR).

**3.  $k < 0$ .** In the general STT the metric (12) describes a wormhole, with two flat asymptotics at  $u = 0$  and  $u = \pi/|k|$ , provided  $\phi$  is regular between them. In exceptional cases the sphere  $u_{\text{max}} = \pi/|k|$  may be an event horizon, namely, if  $\phi \sim 1/\Delta u^2$ ,  $\Delta u \equiv |u - u_{\text{max}}|$ . In this case it has a finite area (a type A black hole) and

$$\omega(\phi) + 3/2 \rightarrow -0 \quad \text{as} \quad u \rightarrow u_{\text{max}}. \quad (21)$$

The behaviour of  $g_{00}$  and  $g_{11}$  near the horizon is then similar to that in the extreme Reissner-Nordström solution.

In the BD theory we have only the wormhole solution

$$\begin{aligned} ds^2 &= e^{-su} \left[ e^{-2bu} dt^2 - \frac{k^2 e^{2bu}}{\sin^2 ku} \left( \frac{k^2 du^2}{\sin^2 ku} + d\Omega^2 \right) \right], \\ s^2(\omega + 3/2) &= -k^2 - 2b^2. \end{aligned} \quad (22)$$

with masses of different signs at the two asymptotics.

For all the BH solutions mentioned, the Hawking temperature is zero. Their infinite horizon areas may mean that their entropy is also infinite; however, a straightforward application of the proportionality relation from GR between entropy and horizon area, is here hardly justified; a calculation of BH entropy is a separate problem, discussed in a large number of recent works from various standpoints.

## 4. Analytic extension and causal structure of Brans-Dicke black holes

### 4.1. Extension

Let us discuss possible Kruskal-like extensions of type B1 BH metrics (17) ( $k > 0$ ) and (20) ( $k = 0$ ) of the BD theory.

For (17), with  $a > 1 > \xi > 2 - a$ , we introduce, as usual, the null coordinates  $v$  and  $w$ :

$$v = t + x, \quad w = t - x, \quad x \stackrel{\text{def}}{=} \int P^{-a} dr \quad (23)$$

where  $x \rightarrow \infty$  as  $r \rightarrow \infty$  and  $x \rightarrow -\infty$  as  $r \rightarrow 2k$ . The asymptotic behaviour of  $x$  as  $r \rightarrow 2k$  ( $P \rightarrow 0$ ) is  $x \propto -P^{1-a}$ , and in a finite neighbourhood of the horizon  $P = 0$  one can write

$$x \equiv \frac{1}{2}(v - w) = -\frac{1}{2}P^{1-a}f(P), \quad (24)$$

where  $f(P)$  is an analytic function of  $P$ , with  $f(0) = 4k/(a - 1)$ :

$$f(P) = -4k \sum_{q=0}^{\infty} \frac{q+1}{q-a+1} P^q. \quad (25)$$

Then, let us define new null coordinates  $V < 0$  and  $W > 0$  related to  $v$  and  $w$  by

$$-v = (-V)^{-n-1}, \quad w = W^{-n-1}, \quad n = \text{const.} \quad (26)$$

The mixed coordinate patch  $(V, w)$  is defined for  $v < 0$  ( $t < -x$ ) and covers the whole past horizon  $v = -\infty$ . Similarly, the patch  $(v, W)$  is defined for  $w > 0$  ( $t > x$ ) and covers the whole future horizon  $w = +\infty$ . So these patches can be used to extend the metric through one or the other horizon.

Consider the future horizon. As is easily verified, a finite value of the metric coefficient  $g_{vW}$  at  $W = 0$  is achieved if we take  $n + 1 = (a - 1)/(1 - \xi)$ , which is positive for  $a > 1 > \xi$ . In a finite neighbourhood of the horizon, the metric (17) can be written in the coordinates  $(v, W)$  as follows:

$$\begin{aligned} ds^2 &= P^{a-\xi} dv dw - P^{1-a-\xi} r^2 d\Omega^2 \\ &= -(n+1) f^{\frac{n+2}{n+1}} \cdot (1 - vW^{n+1})^{-\frac{n+2}{n+1}} dv dW \\ &\quad - \frac{4k^2}{(1-P)^2} f^{-\frac{m}{n+1}} \cdot (1 - vW^{n+1})^{\frac{m}{n+1}} W^{-m} d\Omega^2 \end{aligned} \quad (27)$$

where

$$m = (a - 1 + \xi)/(1 - \xi). \quad (28)$$

The metric (27) can be extended at fixed  $v$  from  $W > 0$  to  $W < 0$  only if the numbers  $n + 1$  and  $m$  are both

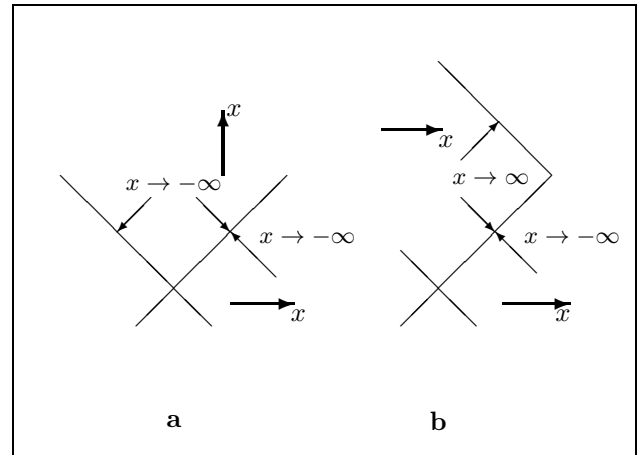


Figure 1: Extensions through the future horizon for odd (a) and even (b) values of  $n$ . Thick vertical and horizontal arrows show the growth direction of the  $x$  coordinate in the corresponding regions.

integers (since otherwise the fractional powers of negative numbers violate the analyticity in the immediate neighbourhood of the horizon). This leads to a discrete set of values of the integration constants  $a$  and  $\xi$ :

$$a = \frac{m+1}{m-n}, \quad \xi = \frac{m-n-1}{m-n}. \quad (29)$$

where, according to the regularity conditions (19),  $m > n \geq 0$ . Excluding the Schwarzschild case  $m = n + 1$  ( $\xi = 0$ ), which corresponds from (22) to  $a = 1$  ( $m = 0$ ), we see that regular BD BHs correspond to integers  $m$  and  $n$  such that

$$m - 2 \geq n \geq 0. \quad (30)$$

An extension through the past horizon can be performed in the coordinates  $(V, w)$  in a similar way and with the same results.

It follows that, although the curvature scalars vanish on the Killing horizon  $P = 0$ , the metric cannot be extended beyond it unless the constants  $a$  and  $\xi$  obey the “quantization condition” (29), and is generically singular. The Killing horizon, which is at a finite affine distance, is part of the boundary of the space-time, i.e. geodesics and other possible trajectories terminate there. Similar properties were obtained in a (2+1)-dimensional model with exact power-law metric functions [11] and in the case of black  $p$ -branes [12].

We have thus obtained a discrete family of BH solutions whose parameters depend on the two integers  $m$  and  $n$ . The corresponding parameters describing the asymptotic form of the solution, the active gravitational mass  $M$  and the scalar charge  $S$ , defined by

$$g_{00} = 1 - \frac{2GM}{r} + o\left(\frac{1}{r}\right), \quad \phi = 1 + \frac{S}{r} + o\left(\frac{1}{r}\right),$$

where  $G$  is the Newtonian gravitational constant, are “quantized” according to the relations

$$GM = k \frac{n+2}{m-n}, \quad S = -2k \frac{m-n-1}{m-n}. \quad (31)$$

The constant  $k$ , specifying the length scale of the solution, remains arbitrary. On the other hand, the coupling constant  $\omega$  takes, according to (18), discrete values:

$$|2\omega + 3| = \frac{(2m-n+1)(n+1)}{(m-n-1)^2}. \quad (32)$$

The  $k=0$  solution (20) of the BD theory also has a Killing horizon ( $u \rightarrow \infty$ ) at finite geodesic distance if  $s > 0$ . However, this space-time does not admit a Kruskal-like extension and so is singular. The reason is that in this case the relation giving the tortoise-like coordinate  $x$ ,

$$x = \int \frac{e^{2bu}}{u^2} du = \frac{e^{2bu}}{2bu^2} F(u) \quad (33)$$

(where  $F(u)$  is some function such that  $F(\infty) = 1$ ) cannot be inverted near  $u = \infty$  to obtain  $u$  as an analytic function of  $x$ .

## 4.2. Geometry and causal structure

To study the geometry beyond the horizons of the metric (17), or (27), let us define the new radial coordinate  $\rho$  by

$$P \equiv e^{-2ku} \equiv 1 - \frac{2k}{r} \equiv \rho^{m-n}. \quad (34)$$

The resulting solution (17), defined in the static region I ( $P > 0$ ,  $\rho > 0$ ), is

$$ds^2 = \rho^{n+2} dt^2 - \frac{4k^2(m-n)^2}{(1-P)^4} \rho^{-n-2} d\rho^2 - \frac{4k^2}{(1-P)^2} \rho^{-m} d\Omega^2, \quad \phi = \rho^{m-n-1}. \quad (35)$$

By (24),  $\rho$  is related to the mixed null coordinates ( $v, W$ ) by

$$\rho(v, W) = W [f(P)]^{1/(n+1)} [1 - vW^{n+1}]^{-1/(n+1)}. \quad (36)$$

This relation and a similar one giving  $\rho(V, w)$  show that when the future (past) horizon is crossed,  $\rho$  varies smoothly, changing its sign with  $W$  ( $V$ ). For  $\rho < 0$  the metric (35) describes the space-time regions beyond the horizons.

To construct the corresponding Penrose diagrams, it is helpful to notice that by (24) the radial coordinate  $x$  is related to  $\rho$  by

$$x = -\frac{1}{2}\rho^{-n-1}f(P), \quad (37)$$

so that for odd  $n$  the horizon as seen from region II ( $\rho < 0$ ) also corresponds to  $x \rightarrow -\infty$ . On the other hand, in the 2-dimensional metric  $ds_2^2 = \rho^{n+2}(dt^2 - dx^2)$ , for  $\rho < 0$  the coordinate  $x$  is timelike, hence in region II beyond the future horizon (with respect to the original region I)  $x \rightarrow -\infty$  means “down”. A new horizon for region II joins the picture at point O — see Fig. 1(a). For even  $n$ , when  $x$  in region II remains a spatial coordinate and the coordinate (37) changes its sign when crossing the horizon, a new horizon joins the old one at the future infinity point of region I — Fig. 1(b). These considerations are easily verified by introducing null coordinates in region II, similar to  $v$  and  $w$  previously used in region I. Continuations through the past horizons are performed in a similar manner. The resulting causal structures depend on the parities of  $m$  and  $n$ .

**1a.** Both  $m$  and  $n$  are even, so  $P(\rho)$  is an even function. The two regions  $\rho > 0$  and  $\rho < 0$  are isometric ( $g_{\mu\nu}(-\rho) = g_{\mu\nu}(\rho)$ ), and the Penrose diagram is similar to that for the extreme Kerr space-time, an infinite tower of alternating regions I and II (Fig. 2, left). All points of the diagram, except the boundary and the horizons, correspond to usual 2-spheres.

**1b.** Both  $m$  and  $n$  are odd; again  $P(\rho)$  is an even function, but regions I and II are now anti-isometric ( $g_{\mu\nu}(-\rho) = -g_{\mu\nu}(\rho)$ ). The metric tensor in region II ( $\rho < 0$ ) has the signature  $(-+++)$  instead of  $(+---)$  in region I. Nevertheless, the Lorentzian nature of the space-time is preserved. The Penrose diagram is shown in Fig. 3, left. In both cases 1a and 1b the maximally extended space-times are globally regular<sup>6</sup>.

**2.**  $m-n$  is odd, i.e.  $P(\rho)$  is an odd function; moreover,  $P \rightarrow -\infty$  ( $r \rightarrow 0$ ) as  $\rho \rightarrow -\infty$ , so that the metric (35) is singular on the line  $\rho = -\infty$ , which is spacelike. The resulting Penrose diagrams are similar to those of the Schwarzschild space-time in case 2a ( $n$  odd,  $m$  even), and of the extreme ( $e^2 = m^2$ ) Reissner–Nordström space-time in case 2b ( $n$  even,  $m$  odd, Fig. 4). In the latter subcase, however, the 4-dimensional metric changes its signature when crossing the horizon, similarly to case 1b.

## 4.3. Type B2 structure

Let us briefly consider the case B2:  $k > 0$ ,  $a > \xi > 1$ . As before, the metric is transformed according to (23)–(26) and at the future null limit (now infinity rather than a horizon, therefore we avoid the term “black

<sup>6</sup>A globally regular extension of an extreme dilatonic black hole, with the same Penrose diagram as in our case 1a, was discussed in [12].

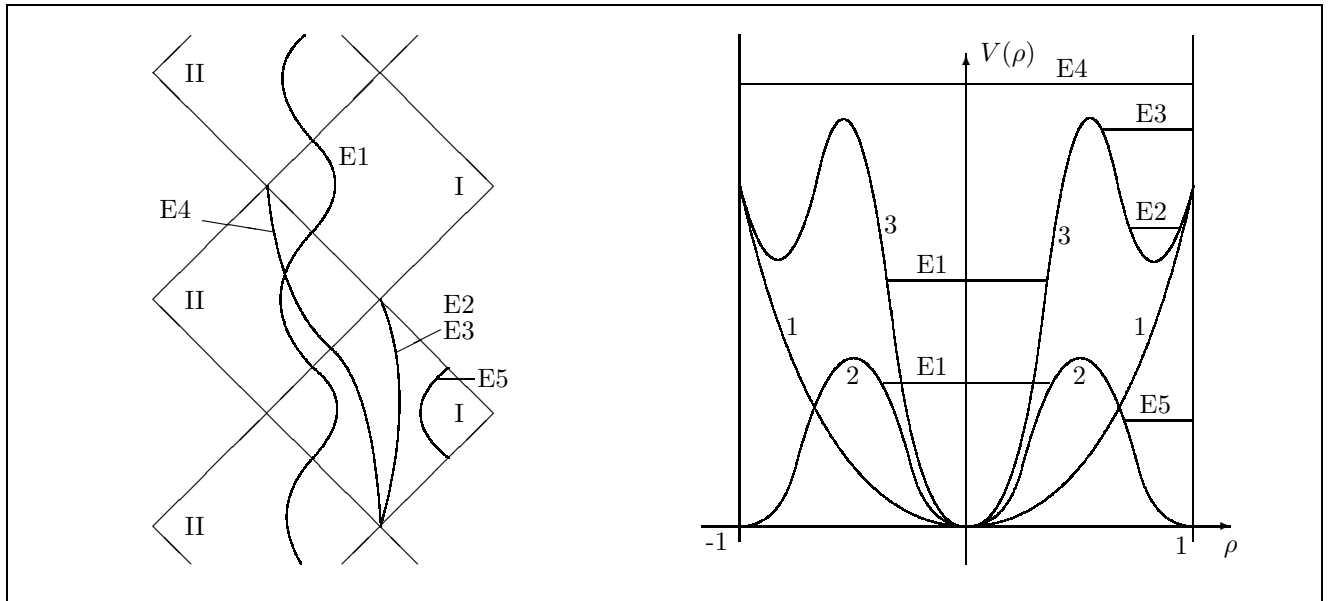


Figure 2: The Penrose diagram and the effective potential for geodesics for a BH with  $m$  and  $n$  both even. Curve 1 is  $V_\eta(\rho)$ , curve 2 is  $V_L(\rho)$  and curve 3 is  $V(\rho)$  for a nonradial timelike geodesic. The curves and “energy levels” E1–E5 correspond to different kinds of geodesics as described in Subsec. 4.4, item 1a.

hole”) we again arrive at (27), where now  $W \rightarrow \infty$  as  $P \rightarrow 0$ . The asymptotic form of the metric as  $W \rightarrow \infty$  is

$$ds^2 = -C_1 dv dW - C_2 W^{-m} d\Omega^2 \quad (38)$$

where  $C_{1,2}$  are some positive constants, while the constant  $m$ , defined in (28), is now negative. A further application of the  $v$ -transformation (26) at the same asymptotic, valid for any finite  $v < 0$ , leads to

$$ds^2 = -C_1(-V)^{(a-\xi)/(\xi-1)} dV dW - C_2 W^{-m} d\Omega^2. \quad (39)$$

If we now introduce new radial ( $R$ ) and time ( $T$ ) coordinates by  $T = V + W$  and  $R = T - W$ , in a spacelike section  $T = \text{const}$  the limit  $R \rightarrow -\infty$  corresponds to simultaneously  $V \rightarrow -\infty$  and  $W \rightarrow +\infty$ , with  $|V| \sim W$ , and the metric (39) turns into

$$ds^2 = 4C_1(-R)^{(a-\xi)/(\xi-1)} (dT^2 - dR^2) - C_2(-R)^{-m} d\Omega^2. \quad (40)$$

Evidently, this asymptotic is a nonflat spatial infinity, with infinitely growing coordinate spheres and also infinitely growing  $g_{00}$ , i.e., this infinity repels test particles.

A Penrose diagram of a B2 type configuration coincides with a single region I in any of the diagrams; all its sides depict null infinities, its right corner corresponds to the usual spatial infinity and its left corner to the unusual one, described by the metric (40). The latter has been obtained here by “moving along” the

future null infinity  $W \rightarrow \infty$ , but the same is evidently achieved starting from the past side.

#### 4.4. Geodesics

Let us now return to type B1 BHs and study test particle motion in their backgrounds, described by geodesics equations.

One can verify that all geodesics are continued smoothly across the horizons, even in cases 1b and 2b when the metric changes its signature (the geodesic equation depends only on the Christoffel symbols and is invariant under the anti-isometry  $g_{\mu\nu} \rightarrow -g_{\mu\nu}$ ).

We will use the metric (35). Then the integrated geodesic equation for arbitrary motion in the plane  $\theta = \pi/2$  reads:

$$\frac{4k^2(m-n)^2}{(1-P)^4} \dot{\rho}^2 + \eta \rho^{n+2} + \frac{L^2}{4k^2} (1-P)^2 \rho^{m+n+2} = E^2 \quad (41)$$

where  $\dot{\rho} \equiv d\rho/d\lambda$ ,  $\lambda$  being an affine parameter such that  $ds^2 = \eta d\lambda^2$ , with  $\eta = +1, 0, -1$  for timelike, null or spacelike geodesics;  $E^2$  and  $L^2$  are constants of motion associated with the timelike and azimuthal Killing vectors and, correspondingly, with the particle total energy and angular momentum. Eq. (41) has the form of an energy balance equation, with the effective potential

$$V(\rho) = V_\eta(\rho) + V_L(\rho) \quad (42)$$

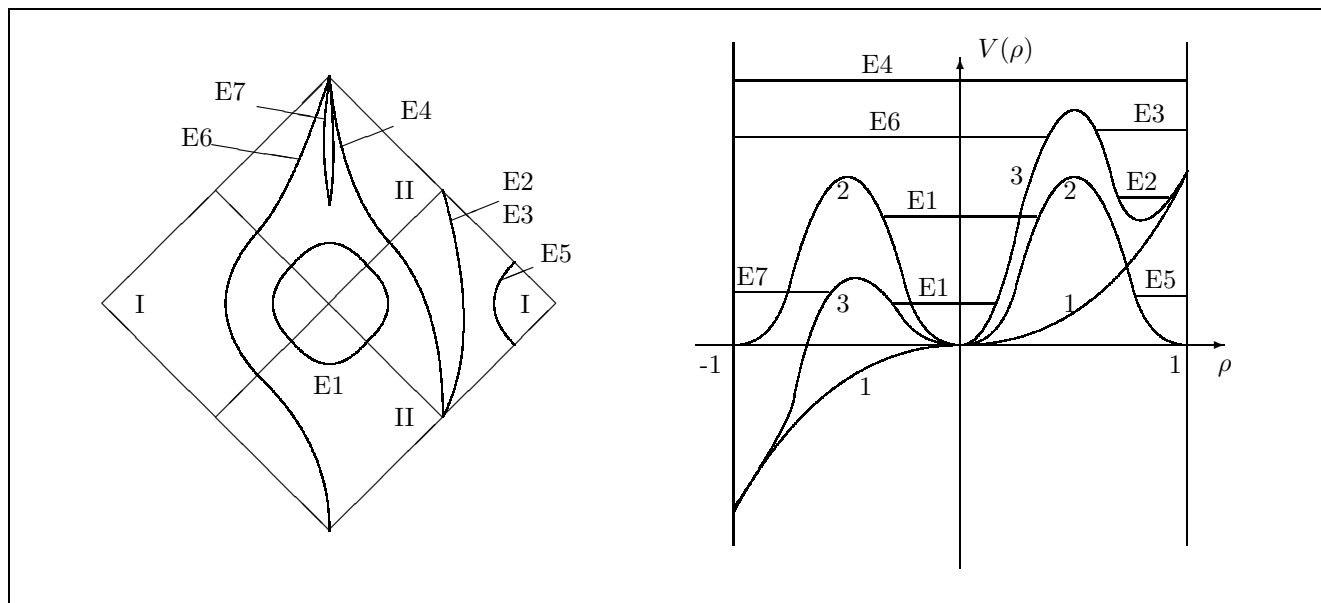


Figure 3: The Penrose diagram and the effective potential for geodesics for a BH with  $m$  and  $n$  both odd. Curve 1 is  $V_\eta(\rho)$ , curve 2 is  $V_L(\rho)$  and curve 3 is  $V(\rho)$  for a nonradial timelike geodesic. The curves and “energy levels” E1–E7 correspond to different kinds of geodesics as described in Subsec. 4.4, item 1b.

where  $V_\eta$  and  $V_L$  are the respective terms in the left-hand side.

One should note that although the coordinate  $\rho$  belongs to the static frame of reference, one can use it (and consequently Eq. (41)) to describe geodesics that cross the horizon since in a close neighbourhood of the horizon  $\rho = 0$  it coincides (up to a positive constant factor) with a manifestly well-behaved coordinate  $V$  or  $W$  and, on the other hand, Eq. (41) reads simply  $\dot{\rho}^2 = \text{const} \cdot E^2$  and is thus also well-behaved.

Let us discuss the four possible cases according to the parity of  $m$  and  $n$  and the corresponding signature of the metric (35) for  $\rho < 0$ :

**1a:**  $m$  even,  $n$  even,  $(+ - - -)$ . The range of  $\rho$  is  $(-1, +1)$ . The coefficient  $(1-P)^{-1}$  of the kinetic term and the potential in (41) are both symmetric under the exchange  $\rho \rightarrow -\rho$ . The potential  $V(\rho)$  is shown in Fig. 2: curve 1 depicts  $V_\eta(\rho)$  for  $\eta = 1$ , i.e., the potential for radial timelike geodesics; curve 2 shows  $V_L$ , the angular momentum dependent part of  $V(\rho)$ , and curve 3 shows their sum for certain generic values of the motion parameters. Depending on the value of  $E$ , geodesic motion can be symmetrical with successive horizon crossings from one region to the next isometrical region without reaching past or future null infinity (E1: see “energy levels” in Fig. 2, right and the corresponding curves in Fig. 2, left), or starting from a past timelike infinity in region I and reaching a future timelike infinity in region II (E4). Some nonradial timelike (E2, E3) and null (E5) geodesics remain in a

single region, corresponding to bound (E2) or unbound (E3) particle orbits near the BH or photons passing it by (E5). The existence of nonradial trajectories like E1 for any value of  $L$  is here connected with the infinite value of  $e^\beta$  at the horizon, creating a minimum of  $V_L$ . Radial null geodesics ( $V(\rho) \equiv 0$ ) correspond, as always, to straight lines tilted by  $45^\circ$  (unshown).

**1b:**  $m$  odd,  $n$  odd,  $(- + + +)$ . The one-dimensional dependence  $\rho(\lambda)$  is qualitatively the same for null geodesics ( $\eta = 0$ ). However, the global picture is drastically different, see Fig. 3. In particular, type E1 null geodesics which periodically cross the horizon necessarily go repeatedly through all four regions of the Penrose diagram, so that their projections onto a 2-dimensional plane  $\theta = \text{const}$ ,  $\Phi = \text{const}$  are closed; they will be even closed in the full 4-dimensional space-time for some discrete values of the angular momentum  $L^2$ . Thus such BH space-times contain closed null geodesics, leading to causality violation.

However, this problem can be avoided if we choose, instead of the simplest, one-sheet maximal analytic extension corresponding to the planar Penrose diagram of Fig. 3, left, a “helical” analytic extension constructed in the following way: starting from a given region I and proceeding with the extension counterclockwise, after 4 steps we come again to a region I isometric to the original one, but do not identify these mutually isometric regions and repeat the process indefinitely. The same process is performed in the clockwise direction. The resulting Penrose diagram is a Riemann sur-

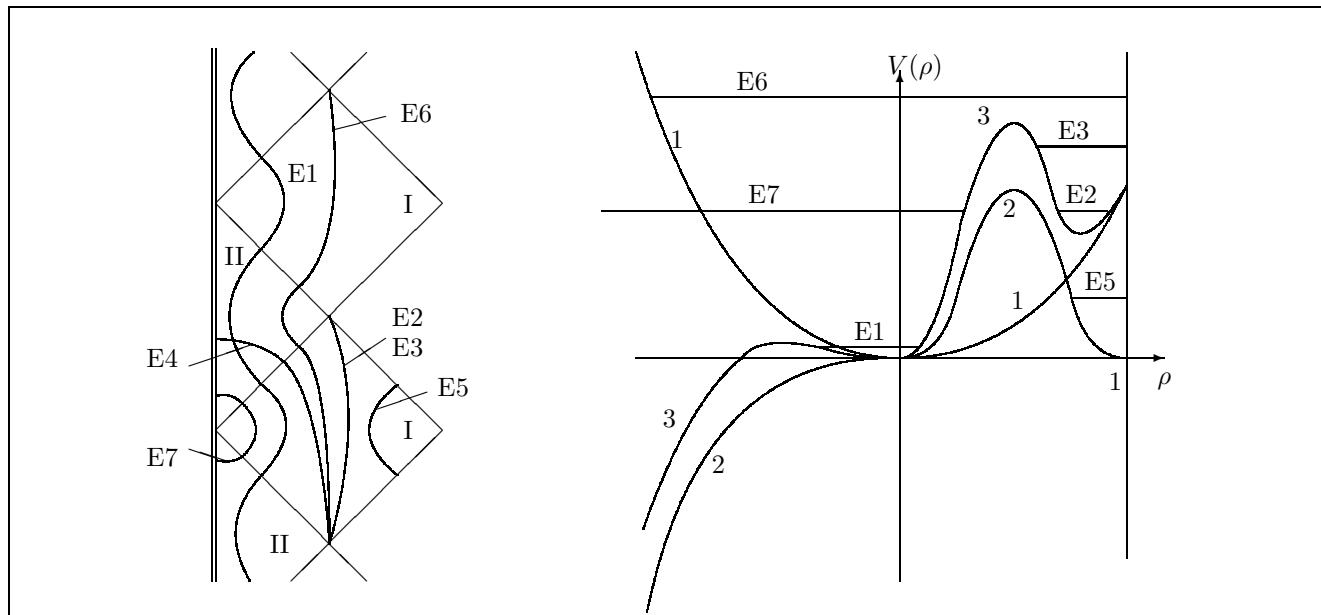


Figure 4: The Penrose diagram and the effective potential for geodesics for a BH with  $n$  even and  $m$  odd. Curve 1 is  $V_\eta(\rho)$ , curve 2 is  $V_L(\rho)$  and curve 3 is  $V(\rho)$  for a nonradial timelike geodesic. The curves and “energy levels” E1–E7 correspond to different kinds of geodesics as described in Subsec. 4.4, item 2b.

face with a countable infinity of sheets similar to that in Fig. 3, left, cut along one of the horizons. Such a structure no longer exhibits causality violation<sup>7</sup>. In general, when crossing a horizon, a null geodesic remains null, but timelike geodesics become spacelike and *vice versa*, since the coefficient  $\eta$  in Eq. (41), being an integral of motion for a given geodesic, changes its meaning in transitions between regions I and II: a geodesic with  $\eta = 1$  is timelike in region I and spacelike in region II, and conversely for  $\eta = -1$ .

For nonnull geodesics the potential is now asymmetric: thus, for trajectories which are timelike in region I ( $\eta = +1$ ), it becomes attractive for  $\rho < 0$  (Fig. 3, the notations coincide with those of Fig. 2). These geodesics become spacelike in region II and generically extend to spacelike infinity as  $\lambda \rightarrow \infty$  (E4 in Fig. 3). This is true for all radial geodesics and part of nonradial ones; however, nonradial geodesics with small E (near the minimum of curve 3 at  $\rho = 0$ ) are of the type E1, quite similar to null E1 trajectories that have been just discussed. A new type of tachyonic motion as compared with item 1a is E6 shown in Fig. 3. There are also circular unstable geodesics with  $\eta = +1$  in region II, with  $t = \text{const}$  and  $\rho = \rho_0 = -[m/(3m - 2n)]^{1/(m-n)}$  (points in the

Penrose diagram), such that  $V(\rho_0) = V'(\rho_0) = 0$ ,  $E = 0$ . All these spacelike geodesics have full analogues with  $\eta = -1$  in region I.

The whole space-time possesses full symmetry under an exchange between regions I and II, corresponding to rotations of the Penrose diagram of Fig. 3 by odd (in addition to even) multiples of the right angle, accompanied by a change of sign of  $\eta$  so that geodesics keep their timelike or spacelike nature.

**2a:**  $m$  even,  $n$  odd,  $(- + - -)$ . The range of  $\rho$  is now  $(-\infty, +1)$ . Both parts of the effective potential become negative and monotonic at  $\rho < 0$ , so that all geodesics entering the horizon terminate at the spacelike singularity  $\rho = -\infty$ , as in the Schwarzschild case. Thus the whole qualitative picture of test particle motion, as well as the Penrose diagram, coincide with the Schwarzschild ones.

**2b:**  $m$  odd,  $n$  even,  $(+ - + +)$ . The potential  $V_\eta$  ( $\eta = 1$ ) is positive-definite (as in the extreme Reissner–Nordström case), as shown in Fig. 4, so that all radial timelike geodesics avoid the singularity, crossing the horizon either twice (E6), or indefinitely (E1). For nonradial motion, the summed potential  $V(\rho) \rightarrow -\infty$  as  $\rho \rightarrow -\infty$ , whatever small is  $L^2$ , therefore all geodesics that are timelike in region I (and become spacelike in region II) reach the spacelike singularity<sup>8</sup>  $\rho = -\infty$

<sup>7</sup>Strictly speaking, such a process might be applied to the Schwarzschild and Rindler space-times, with possible identification of isometric regions after a finite number of steps. This is, however, unnecessary since there a causality problem like ours does not exist.

<sup>8</sup>Due to the metric signature change, in the Penrose diagram of Fig. 4, just as in Fig. 3 for the case 1b, the time direction is vertical in regions I and horizontal in regions II.



(levels and curves E4 and E7 in Fig. 4), except those with small  $E$  depicted as E1.

One can conclude that the unusual nature of metric of B1 type BHs creates some unusual types of particle motion. Some of them even exhibit evident causality violation — such as an observer receiving messages from his or her own future — which can be avoided by assuming a more complicated space-time structure.

Another paradox, also related to causality, arises if we follow in cases 1b or 2b the fate of a hypothetical (timelike) observer who has crossed the horizon and finds him(her)self in a region II where his (her) proper time is now spacelike as viewed by a resident observer (whose timelike geodesic is entirely contained in region II), and can be reversed by a simple coordinate change.

However, one may suspect that, the horizon area being infinite, any extended body, and an observer in particular, will have been infinitely stretched apart and destroyed before actually crossing the horizon. To check this, consider for instance a freely falling observer whose center of mass follows a radial geodesic in the plane  $\theta = \pi/2$ . The separation  $n^\alpha$  between this geodesic and a neighbouring radial geodesic varies according to the law of geodesic deviation

$$\frac{D^2 n^\alpha}{d\lambda^2} + R^\alpha{}_{\beta\gamma\delta} u^\beta n^\gamma u^\delta = 0. \quad (43)$$

For the four-velocity of the center of mass we have  $u^0 = E g^{00}$  and  $u^0 u_0 + u^1 u_1 = 1$ , so that near the horizon  $u^\mu \simeq (E g^{00}, E(-g^{00} g^{11})^{1/2}, 0, 0)$ . We obtain for the relative azimuthal acceleration near the horizon

$$\begin{aligned} \frac{1}{n^3} \frac{D^2 n^3}{d\lambda^2} &= (R^{30}{}_{30} u^0 u_0 + R^{31}{}_{31} u^1 u_1) \\ &\simeq -E^2 g^{00} (R^{30}{}_{30} - R^{31}{}_{31}) = E^2 R''/R, \end{aligned} \quad (44)$$

and a similar equation for the deviation  $n^2$  in the  $\theta$  direction. Here  $R^2 = |g_{22}|$ ,  $R'' = d^2 R/d\rho^2$ , and  $\rho$  is a radial coordinate such that the Jordan-frame metric functions are related by  $g_{00} g_{11} = \text{const}$ ; this condition is valid near the horizon for our coordinate  $\rho$  defined in (34).

The azimuthal geodesic deviation (44) which, due to its structure, is insensitive to radial boosts and is thus equally applicable to the static frame of reference and to the one comoving with the infalling body, agrees with similar relations given by Horowitz and Ross [13]. In the case of the Schwarzschild metric,  $R''/R = 0$  and the tidal force (given by the terms that we have neglected) is finite. In the case of the examples discussed in [13],  $R''/R$  is negative and large, i.e. geodesics converge and physical bodies are crushed as they approach the horizon, as by a naked singularity, hence the name “naked black holes” given to these spacetimes in [13]. On the contrary, in the case of the cold black hole

metric (35),  $R''/R \rightarrow +\infty$  (as  $\rho^{-2}$ ), i.e. geodesics diverge; the resulting infinite tidal forces pull apart all extended objects, e.g. any kind of clock, approaching the horizon. Only true elementary (pointlike) particles, resulting from the destruction of the falling body, cross such a horizon to become tachyons<sup>9</sup>.

## 5. Stability

Let us now study small (linear) spherically symmetric perturbations of the above static solutions (or static regions of the BHs), i.e. consider, instead of  $\varphi(u)$ ,

$$\varphi(u, t) = \varphi(u) + \delta\varphi(u, t) \quad (45)$$

and similarly for the metric functions  $\alpha, \beta, \gamma$ , where  $\varphi(u)$ , etc., are taken from the static solutions of Sec. 2. We are working in the Einstein conformal frame and use Eqs. (4). The consideration applies to the whole class of STT (1); its different members can differ in boundary conditions, to be discussed below.

In perturbation analysis there is the so-called gauge freedom, i.e. that of choosing the frame of reference and the coordinates of the perturbed space-time. The most frequently used frame for studying radial perturbations has been that characterized by the technically convenient condition  $\delta\beta \equiv 0$  [10, 14, 15]. It was applied, however, to background configurations where the area function  $e^\beta$  was monotonic in the whole range of  $u$ , or was itself used as a coordinate in the static space-time. Unlike that, in our study the configurations of utmost interest are type B black holes and wormholes, i.e. those having a minimum of  $e^\beta$  (a throat) at some value of  $u$  and infinite  $e^\beta$  at both ends of the  $u$  range. At the throats, the equality  $\delta\beta \equiv 0$  is no longer a coordinate condition, but a physical restriction, forcing the throat to be at rest. It can be explicitly shown that the condition  $\delta\beta \equiv 0$  creates poles in the effective potential for perturbations, leading to their separate existence at different sides of the throat, i.e. the latter behaves like a wall.

For these reasons, we have to use another gauge, and we choose it in the form

$$\delta\alpha = 2\delta\beta + \delta\gamma, \quad (46)$$

extending to perturbations the harmonic coordinate condition of the static system. In this and only in this case the scalar equation (11) for  $\delta\varphi$  decouples from the other perturbation equations and reads

$$e^{4\beta(u)} \delta\ddot{\varphi} - \delta\varphi'' = 0. \quad (47)$$

<sup>9</sup>Our cold black holes are thus counterexamples to the claim made in [13] that a smooth extension is not possible when tidal forces diverge on the horizon.

Since the scalar field is the only dynamical degree of freedom, this equation can be used as the master one, while others only express the metric variables in terms of  $\delta\varphi$ , provided the whole set of field equations is consistent. That it is indeed the case, can be verified directly. Indeed, under the condition (46), the four equations (7)–(10) for perturbations take the form

$$e^{4\beta}(4\delta\beta + \delta\gamma)' - \delta\gamma'' = 0; \quad (48)$$

$$e^{4\beta}(2\delta\beta + \delta\gamma)' - 2\delta\beta'' - \delta\gamma'' - 4(\beta' - \gamma')\delta\beta' + 4\beta'\delta\gamma' = 2\varepsilon\varphi'\delta\varphi'; \quad (49)$$

$$e^{4\beta}\delta\ddot{\beta} - \delta\beta'' + 2e^{2\beta+2\gamma}(\delta\beta + \delta\gamma) = 0; \quad (50)$$

$$\dot{\beta}' - \beta'(\delta\beta + \delta\gamma)' - \gamma'\delta\dot{\beta} = -\frac{1}{2}\varepsilon\varphi'\delta\dot{\varphi}, \quad (51)$$

where  $\alpha, \beta, \gamma, \varphi$  satisfy the static field equations.

Eq. (51) may be integrated in  $t$  and further differentiated in  $u$ ; the result turns out to be proportional to a linear combination of the remaining Einstein equations (48)–(50). On the other hand, the quantities  $\delta\dot{\varphi}$  and  $\delta\varphi''$  can be calculated from (48)–(51), resulting in (47). Therefore we have three independent equations for the three functions  $\delta\varphi, \delta\beta$  and  $\delta\gamma$ .

The following stability analysis rests on Eq. (47). The static nature of the background solution makes it possible to separate the variables,

$$\delta\varphi = \psi(u) e^{i\omega t}, \quad (52)$$

and to reduce the stability problem to a boundary-value problem for  $\psi(u)$ . Namely, if there exists a non-trivial solution to (47) with  $\omega^2 < 0$ , satisfying some physically reasonable boundary conditions at the ends of the range of  $u$ , then the static background system is unstable since perturbations can exponentially grow with  $t$ . Otherwise it is stable in the linear approximation.

Suppose  $-\omega^2 = \Omega^2, \Omega > 0$ . In what follows we use two forms of the radial equation (47): the one directly following from (52),

$$\psi'' - \Omega^2 e^{4\beta(u)}\psi = 0, \quad (53)$$

and the normal Liouville (Schrödinger-like) form

$$d^2y/dx^2 - [\Omega^2 + V(x)]y(x) = 0, \quad (54)$$

$$V(x) = e^{-4\beta}(\beta'' - \beta'^2).$$

obtained from (53) by the transformation

$$\psi(u) = y(x) e^{-\beta}, \quad x = - \int e^{2\beta(u)} du. \quad (55)$$

Here, as before, a prime denotes  $\partial/\partial u$ .

The boundary condition at spatial infinity ( $u \rightarrow 0, x \simeq 1/u \rightarrow +\infty$ ) is evident:  $\delta\varphi \rightarrow 0$ , or  $\psi \rightarrow 0$ . For our metric (12) the effective potential  $V(x)$  has the asymptotic form

$$V(x) \approx 2b/x^3, \quad \text{as} \quad x \rightarrow +\infty, \quad (56)$$

hence the general solutions to (54) and (53) have the asymptotic form

$$y \sim c_1 e^{\Omega x} + c_2 e^{-\Omega x} \quad (x \rightarrow +\infty), \quad (57)$$

$$\psi \sim u(c_1 e^{\Omega/u} + c_2 e^{-\Omega/u}) \quad (u \rightarrow 0), \quad (58)$$

with arbitrary constants  $c_1, c_2$ . Our boundary condition leads to  $c_1 = 0$ .

For  $u \rightarrow u_{\max}$ , where in many cases the background field  $\varphi$  tends to infinity, a formulation of the boundary condition is not so evident. Refs. [14, 15] and others, dealing with minimally coupled or dilatonic scalar fields, used the minimal requirement providing the validity of the perturbation scheme in the Einstein frame:

$$|\delta\varphi/\varphi| < \infty. \quad (59)$$

In STT, where Jordan-frame and Einstein-frame metrics are related by  $g_{\mu\nu}^J = (1/\phi)g_{\mu\nu}^E$ , it seems reasonable to require that the perturbed conformal factor  $1/\phi$  behave no worse than the unperturbed one, i.e.

$$|\delta\phi/\phi| < \infty. \quad (60)$$

An explicit form of this requirement depends on the specific STT and can differ from (59), for example, in the BD theory, where  $\phi$  and  $\varphi$  are connected by (5), the requirement (60) leads to  $|\delta\varphi| < \infty$ . We will refer to (59) and (60) as to the “weak” and “strong” boundary condition, respectively. For configurations with regular  $\phi$  and  $\varphi$  at  $u \rightarrow u_{\max}$  these conditions both give  $|\delta\varphi| < \infty$ .

Let us now discuss different cases of the STT solutions. We will suppose that the scalar field  $\phi$  is regular for  $0 < u < u_{\max}$ , so that the conformal factor  $\phi^{-1}$  in (12) does not affect the range of the  $u$  coordinate.

**1.**  $\varepsilon = +1, k > 0$ . This is the singular solution of normal STT. As  $u \rightarrow +\infty, \beta \sim (b-k)u \rightarrow -\infty$ , so that  $x$  tends to a finite limit and with no loss of generality one can put  $x \rightarrow 0$ . The effective potential  $V(x)$  then has a negative double pole,  $V \sim -1/(4x^2)$ , and the asymptotic form of the general solution to (54) leads to

$$\psi(u) \approx y(x)/\sqrt{x} \approx (c_3 + c_4 \ln x) \quad (x \rightarrow 0). \quad (61)$$

The weak boundary condition leads to the requirement  $|\delta\varphi/\varphi| \approx |y|/(\sqrt{x}|\ln x|) < \infty$ , met by the general solution (61) and consequently by its special solution that joins the allowed case ( $c_1 = 0$ ) of the solution (57) at the spatial asymptotic. We then conclude that the static field configuration is unstable, in agreement with the previous work [14].

As for the strong boundary condition (60), probably more appropriate in STT, its explicit form varies from theory to theory, therefore a general conclusion

cannot be made. In the special case of the BD theory the condition (60) means  $|\psi| < \infty$  as  $u \rightarrow +\infty$ . Such an asymptotic behavior is forbidden by (Eq. (53), according to which  $\psi''/\psi > 0$ , i.e. the perturbation  $\psi(u)$  is convex and so cannot be bounded as  $u \rightarrow \infty$  for an initial value  $\psi(0) = 0$  ( $c_1 = 0$ ). We thus conclude that the static system is stable.

We see that in this singular case the particular choice of a boundary condition is crucial for the stability conclusion. In the case of GR with a minimally coupled scalar field [14] there is no reason to “strengthen” the weak condition that leads to the instability. In the BD case the strong condition seems more reasonable, so that the BD singular solution seems stable. For any other STT the situation must be considered separately.

**2.**  $\varepsilon = -1$ ,  $k > 0$ . This case includes some singular solutions and cold black holes, as is exemplified for the BD theory in (17)–(19).

As  $u \rightarrow +\infty$ ,  $\beta \sim (b - k)u \rightarrow +\infty$ , so that  $x \rightarrow -\infty$  and  $V(x) \approx -1/(4x^2) \rightarrow 0$ . The general solution to Eq. (54) again has the asymptotic form (57) for  $x \rightarrow -\infty$ . The weak condition (59) leads, as in the previous case, to the requirement  $|y|/(\sqrt{|x|} \ln|x|) < \infty$ , and, applied to (57), to  $c_2 = 0$ . This means that the function  $\psi$  must tend to zero for both  $u \rightarrow 0$  and  $u \rightarrow \infty$ , which is impossible due to  $\psi''/\psi > 0$ . Thus the static system is stable. Obviously the more restrictive strong condition (60) can only lead to the same conclusion.

**3.**  $\varepsilon = -1$ ,  $k = 0$ . There are again singular solutions and cold black holes. As  $u \rightarrow +\infty$ ,  $x \rightarrow -\infty$  and again the potential  $V(x) \approx -1/4x^2 \rightarrow 0$ , leading to the same conclusion as in case 2.

**4.**  $\varepsilon = -1$ ,  $k < 0$ . In the generic case the solution describes a wormhole, and in the exceptional case (21) there is a cold black hole with a finite horizon area. In all such cases, as  $u \rightarrow u_{\max} = \pi/|k|$ , one has  $x \rightarrow -\infty$  and  $V \sim 1/|x|^3 \rightarrow 0$ , so that the stability is concluded just as in cases 2 and 3.

Thus, generically, scalar-vacuum spherically symmetric solution of anomalous STT are linearly stable against spherically symmetric perturbations. Excluded are only the cases when the field  $\phi$  behaves in a singular way inside the coordinate range  $0 < u < u_{\max}$ ; such cases should be studied individually.

### Acknowledgement

This work was supported in part by CNPq (Brazil) and CAPES (Brazil).

### References

- [1] D. Kaiser, *Phys. Rev.* **D 15**, 4295 (1995); J. Hwang, “The Origin of Structure in Generalized Gravity”, gr-qc/9711067.
- [2] M. Campanelli and C.O. Lousto, *Int. J. Mod. Phys.* **D 2**, 451 (1993).
- [3] K.A. Bronnikov, C.P. Constantinidis, R.L. Evangelista and J.C. Fabris, “Cold Black Holes in Scalar-Tensor Theories”, *preprint* PDF-UFES 001/97, gr-qc/9710092.
- [4] K.A. Bronnikov, *Acta Phys. Polon.* **B 4**, 251 (1973).
- [5] C.M. Will, “Theory and Experiment in Gravitational Physics”, Cambridge University Press, Cambridge, 1993.
- [6] K.A. Bronnikov, *Grav. & Cosmol.* **2**, 221 (1996).
- [7] K.A. Bronnikov, G. Clément, C.P. Constantinidis and J.C. Fabris, *Phys. Lett. A*, to be published; gr-qc/9801050.
- [8] N.M. Bocharova, K.A. Bronnikov and V.N. Melnikov, *Vestn. Mosk. Univ., Fiz. Astron.*, No. 6, 706 (1970).
- [9] J.D. Bekenstein, *Ann. Phys. (NY)* **82**, 535 (1974).
- [10] K.A. Bronnikov and Yu.N. Kireyev, *Phys. Lett. A* **67**, 95 (1978).
- [11] G. Clément and A. Fabbri, “The Gravitating  $\sigma$  Model in 2+1 Dimensions: Black Hole Solutions”, *preprint* GCR-98/04/01, gr-qc/9804050.
- [12] G.W. Gibbons, G.T. Horowitz and P.K. Townsend, *Class. Quantum Grav.* **12**, 297 (1995).
- [13] G.T. Horowitz and S.F. Ross, *Phys. Rev.* **D 56**, 2180 (1997); **D 57**, 1098 (1998).
- [14] K.A. Bronnikov and A.V. Khodunov, *Gen. Rel. & Grav.* **11**, 13 (1979).
- [15] K.A. Bronnikov and V.N. Melnikov, *Ann. Phys. (NY)* **239**, 40 (1995).